51st IEEE Conference on Decision and Control
December 10-13, 2012. Maui, Hawaii, USA

Robust Sampled-Data Adaptive Control of the Rohrs Counterexamples

E. Dogan Sumer, Dennis S. Bernstein

Department of Aerospace Engineering, University of Michigan, 1320 Beal Ave., Ann Arbor, MI 48109

***Abstract*— We revisit the Rohrs counterexamples within the context of sampled-data adaptive control. In particular, retrospective cost adaptive control (RCAC) is applied to the sampled continuous-time plant with unmodeled high-frequency dynamics, which involves nonminimum-phase (NMP) sampling zeros. It is shown that, without knowledge of these NMP zeros, RCAC stabilizes the uncertain plant and asymptotically follows the sinusoidal command.**

I. Introduction

The history of adaptive control is marked by two key events. The first was the tragic accident in 1967 involving the X-15. The second was the publication in 1982 of [1], which presented two counterexamples showing the fragility of model reference adaptive control (MRAC) schemes. These counterexamples considered plants with high-frequency unmodeled dynamics that can induce a large, unknown phase shift in the plant's open-loop response leading to unbounded response. These events dampened enthusiasm for adaptive control and led to a cautionary view of these techniques [2, 3]. Nevertheless, adaptive control continued to be developed and applied to a vast range of applications [4–6].

The purpose of the present paper is to revisit both Rohrs counterexamples using retrospective cost adaptive control (RCAC). RCAC is a discrete-time, direct adaptive control technique that can be used for plants that are possibly MIMO, nonminimum phase (NMP), and unstable [7–11]. This approach relies on knowledge of Markov parameters and, for NMP open-loop-unstable plants, estimates of the NMP zeros. For SISO systems that are either open-loop asymptotically stable or minimum phase, a single Markov parameter typically suffices. This information can be obtained from either analytical modeling or system identification [12]. Alternatively, an identified FIR model based on phase matching can be used [11, 13, 14]

The goal of the present paper is thus to apply sampled-data adaptive control to the Rohrs counterexamples. From a sampled-data point of view, the challenging aspect of these problems for RCAC is not the unmodeled dynamics per se, but rather the sampling zeros, which may be NMP under fast sampling. Since the Rohrs counterexamples are open-loop asymptotically stable, RCAC is able to provide reliable performance without knowledge of either the unmodeled high-frequency dynamics or the NMP sampling zeros [11].

II. Problem Formulation

Consider the MIMO discrete-time system

$$x(k+1) = Ax(k) + Bu(k) + D_1 w(k), \tag{1}$$

$$y(k) = Cx(k) + D_2 w(k), \tag{2}$$

$$z(k) = E_1 x(k) + E_0 w(k), \tag{3}$$

where $k \geq 0$, $x(k) \in \mathbb{R}^n$, $z(k) \in \mathbb{R}^{l_z}$ is the measured performance variable to be minimized, $y(k) \in \mathbb{R}^{l_y}$ contains additional measurements that are available for control, $u(k) \in \mathbb{R}^{l_u}$ is the input signal, $w(k) \in \mathbb{R}^{l_w}$ is the exogenous signal that can represent either a reference command, an external disturbance, or both. The system (1)–(3) can represent a sampled-data application arising from a continuous-time system with sample and hold operations with the sampling period h, where $y(k)$ represents $y(kh)$, $z(k)$ represents $z(kh)$, and so on. The operator matrix from u to z is thus given by

$$G_{zu}(\mathbf{q}) \triangleq E_1(\mathbf{q}I - A)^{-1}B, \tag{4}$$

where $\mathbf{q}$ is the shift operator which accounts for possibly nonzero initial conditions. Furthermore, for a positive integer i, $H_i \triangleq E_1 A^{i-1} B$ is the i^{th} Markov parameter of G_{zu}.

Now, consider the output-feedback controller

$$x_{\mathrm{c}}(k+1) = A_{\mathrm{c}}(k)x_{\mathrm{c}}(k) + B_{\mathrm{c}}(k)y(k), \tag{5}$$

$$u(k) = C_{\mathrm{c}}(k)x_{\mathrm{c}}(k), \tag{6}$$

where $x_{\mathrm{c}} \in \mathbb{R}^{n_{\mathrm{c}}}$. The closed-loop system with output feedback (5), (6) is thus given by

$$\tilde{x}(k+1) = \tilde{A}(k)\tilde{x}(k) + \tilde{D}_1(k)w(k), \tag{7}$$

$$y(k) = \tilde{C}\tilde{x}(k) + D_2 w(k), \tag{8}$$

$$z(k) = \tilde{E}_1\tilde{x}(k) + E_0 w(k), \tag{9}$$

where $\tilde{x} \triangleq \left[\begin{array}{cc} x^{\mathrm{T}} & x_c^{\mathrm{T}} \end{array}\right]^{\mathrm{T}}$,

$$\tilde{A}(k) = \left[\begin{array}{cc} A & BC_{\mathrm{c}}(k) \\ B_{\mathrm{c}}(k)C & A_{\mathrm{c}}(k) \end{array}\right], \tilde{D}_1(k) = \left[\begin{array}{c} D_1 \\ B_{\mathrm{c}}(k)D_2 \end{array}\right],$$

$$\tilde{C} = \left[\begin{array}{cc} C & 0_{l_y \times n_{\mathrm{c}}} \end{array}\right], \quad \tilde{E}_1 = \left[\begin{array}{cc} E_1 & 0_{l_z \times n_{\mathrm{c}}} \end{array}\right].$$

The goal is to develop an adaptive output feedback controller to minimize the performance measure $z^{\mathrm{T}}z$ in the presence of the exogenous signal w with limited modeling information about the dynamics and exogenous signal.

The model reference adaptive control (MRAC) problem can be formulated in terms of (1)–(3), where $z \triangleq y_0 - y_{\mathrm{m}}$ is the command-following error between the plant output y_0

and the output $y_{\rm m}$ of a reference model $G_{\rm m}$ whose input is the reference signal r. For MRAC, the measurement of the reference signal r is assumed to be available for feedforward compensation, as shown in Figure 1.

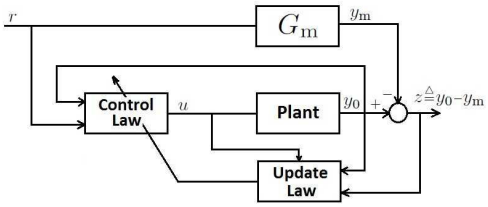

Fig. 1. MRAC Problem

For the adaptive controller (5), (6), the closed-loop state matrix $\tilde{A}(k)$ may be time-varying. To monitor the ability of the adaptive controller to stabilize the plant, we compute the spectral radius $\mathrm{spr}(\tilde{A}(k))$ at each time step. If the controller converges, and $\mathrm{spr}(\tilde{A}(k))$ converges to a number less than 1, then the asymptotic closed-loop system is internally stable.

III. Retrospective Cost Adaptive Control

We represent (5), (6) by

$$u(k) = \theta^{\mathrm{T}}(k)\phi(k-1), \tag{10}$$

where $\phi(k-1) = \left[\, y^{\mathrm{T}}(k-1) \;\cdots\; y^{\mathrm{T}}(k-n_{\rm c}) \;\, u^{\mathrm{T}}(k-1) \;\cdots\; u^{\mathrm{T}}(k-n_{\rm c}) \,\right]^{\mathrm{T}}$, $\theta(k) = \left[\, N_1^{\mathrm{T}}(k) \;\cdots\; N_{n_{\rm c}}^{\mathrm{T}}(k) \;\, M_1^{\mathrm{T}}(k) \;\cdots\; M_{n_{\rm c}}^{\mathrm{T}}(k) \,\right]^{\mathrm{T}}$, and, for all $1 \le i \le n_{\rm c}$, $N_i(k) \in \mathbb{R}^{l_y \times l_u}$, $M_i(k) \in \mathbb{R}^{l_u \times l_u}$. The control law (10) can be reformulated as

$$u(k) = \Phi(k-1)\Theta(k), \tag{11}$$

where $\Phi(k-1) \triangleq I_{l_u} \otimes \phi^{\mathrm{T}}(k-1) \in \mathbb{R}^{l_u \times l_u n_{\rm c}(l_u+l_y)}$, and $\Theta(k) \triangleq \mathrm{vec}(\theta(k)) \in \mathbb{R}^{l_u n_{\rm c}(l_u+l_y)}$.

Now, for a positive integer r, we define the finite-impulse-response (FIR) transfer matrix

$$G_{\rm f}(\mathbf{q}) \triangleq \frac{K_1\mathbf{q}^{r-1} + K_2\mathbf{q}^{r-2} + \cdots + K_r}{\mathbf{q}^r}, \tag{12}$$

where $K_i \in \mathbb{R}^{l_z \times l_u}$ for $1 \le i \le r$. Next, for $k \ge 1$, we define the *retrospective performance variable*

$$\hat{z}(\hat{\Theta}(k), k) \triangleq z(k) + \Phi_{\rm f}(k-1)\hat{\Theta}(k) - u_{\rm f}(k), \tag{13}$$

with

$$\Phi_{\rm f}(k-1) \triangleq G_{\rm f}(\mathbf{q})\Phi(k-1) \in \mathbb{R}^{l_z \times l_u n_{\rm c}(l_u+l_y)}, \tag{14}$$

$$u_{\rm f}(k) \triangleq G_{\rm f}(\mathbf{q})u(k) \in \mathbb{R}^{l_z}, \tag{15}$$

where $\hat{\Theta}(k)$ will be determined by optimization below.

For $k > 0$, we define the cumulative cost function

$$\begin{aligned} J(\hat{\Theta}(k), k) \triangleq & \sum_{i=1}^{k} \lambda^{k-i} \hat{z}^{\mathrm{T}}(\hat{\Theta}(k), i)\hat{z}(\hat{\Theta}(k), i) \\ & + \sum_{i=1}^{k} \lambda^{k-i}\eta(i)\hat{\Theta}^{\mathrm{T}}(k)\Phi_{\rm f}^{\mathrm{T}}(i-1)\Phi_{\rm f}(i-1)\hat{\Theta}(k) \\ & + \lambda^k(\hat{\Theta}(k) - \Theta_0)^{\mathrm{T}}P_0^{-1}(\hat{\Theta}(k) - \Theta_0), \end{aligned} \tag{16}$$

where $\lambda \in (0, 1]$, P_0 is positive definite, and $\eta(k) \ge 0$. In this paper, we choose

$$\eta(k) \triangleq \eta_0 \sum_{j=0}^{p_c-1} z^{\mathrm{T}}(k-j)z(k-j). \tag{17}$$

where $\eta_0 \ge 0$, and $p_c \ge 1$. The following result, which follows from RLS theory [4, 5], provides the global minimizer of the cost function (16) and thus the update law.

Proposition 3.1: Let $P(0) = P_0$ and $\Theta(0) = \Theta_0$. Then, for all $k \ge 1$, the cumulative cost function (16) has a unique global minimizer $\Theta(k)$. Furthermore, $\Theta(k)$ is given by

$$\begin{aligned} \Theta(k) = & \left[I - K(k)\Phi_{\rm f}(k-1)\right]\Theta(k-1) \\ & - P(k)\Phi_{\rm f}^{\mathrm{T}}(k-1)\left[z(k) - u_{\rm f}(k)\right], \end{aligned}$$

where $P(k)$ satisfies

$$P(k) = \frac{1}{\lambda}\left[P(k-1) - K(k)\Phi_{\rm f}(k-1)P(k-1)\right],$$

and

$$\begin{aligned} K(k) \triangleq & P(k-1)\Phi_{\rm f}^{\mathrm{T}}(k-1) \\ & \cdot \left[\frac{\lambda}{1+\eta(k)}I_{l_z} + \Phi_{\rm f}(k-1)P(k-1)\Phi_{\rm f}^{\mathrm{T}}(k-1)\right]^{-1} \end{aligned}$$

IV. Construction of $G_{\rm f}$

In this section, we discuss two methods for constructing $G_{\rm f}$. Since the Rohrs counterexamples are the focus of this paper, we limit the discussion to SISO plants.

A. NMP-Zero-Based Construction of $G_{\rm f}$

We rewrite (4) as $G_{zu}(\mathbf{q}) = H_d\frac{N(\mathbf{q})}{D(\mathbf{q})}$, where $D(\mathbf{q})$ is a monic polynomial of degree n, $N(\mathbf{q})$ is a monic polynomial of degree $n-d$, and d is the relative degree of G_{zu}. Assume that H_d and the nonminimum-phase (NMP) zeros of G_{zu}, if any, are known. Now, consider the numerator factorization

$$N(\mathbf{q}) = \beta_{\rm U}(\mathbf{q})\beta_{\rm S}(\mathbf{q}), \tag{18}$$

where $\beta_{\rm U}(\mathbf{q})$ and $\beta_{\rm S}(\mathbf{q})$ are monic polynomials of orders $n_{\rm U}$ and $n_{\rm S} = n - d - n_{\rm U}$, respectively, and each NMP zero of $G_{zu}(\mathbf{q})$ is a root of $\beta_{\rm U}(\mathbf{q})$. The NMP-zero-based construction of $G_{\rm f}$ is given by

$$G_{\rm f}(\mathbf{q}) = H_d\frac{\beta_{\rm U}(\mathbf{q})}{\mathbf{q}^{n_{\rm U}+d}}. \tag{19}$$

Robustness of this construction is discussed in [8] for minimum-phase systems, where it is shown that RCAC has 6-dB downward gain margin, and infinite upward gain margin to uncertainty in H_d. Finally, this construction does not require $\eta_0 > 0$ in (17) as long as $G_{\rm f}$ captures the NMP zeros of G_{zu}.

B. Phase-Matching-Based Construction of $G_{\rm f}$

For $\Omega \in [0, \pi]$ rad/sample, consider the *phase mismatch* $\Delta(\Omega)$ between $G_{\rm f}$ and G_{zu} defined by

$$\Delta(\Omega) \triangleq \cos^{-1}\frac{\mathrm{Re}\left[G_{zu}(e^{\jmath\Omega})\overline{G_{\rm f}(e^{\jmath\Omega})}\right]}{|G_{zu}(e^{\jmath\Omega})|\,|G_{\rm f}(e^{\jmath\Omega})|} \in [0, 180]. \tag{20}$$

Note that $\Delta(\Omega)$ represents the angle between $G_{zu}(e^{\jmath\Omega})$ and $G_{\rm f}(e^{\jmath\Omega})$ in the complex plane. For the phase-mismatch-based construction, $G_{\rm f}$ is chosen to satisfy

$$\Delta(\Omega) \leq 90 \text{ deg}, \text{for all } \Omega \in [0,\ \pi] \text{ rad/sample}. \quad (21)$$

A weaker condition is sufficient when G_{zu} is asymptotically stable, and the exogenous signal $w(k)$ is harmonic. In this case, the phase-mismatch-based construction requires

$$\Delta(\Omega) \leq 90 \text{ deg}, \Omega \in \text{spec}(w), \quad (22)$$

where "spec(w)" is the frequency spectrum of w.

The phase-matching-based construction of $G_{\rm f}$ is applicable to plants that are either minimum-phase or Lyapunov stable, that is, plants that are not both unstable and NMP. For NMP systems, this construction requires that η_0 be positive.

The robustness of the phase-matching-based construction to phase mismatch is addressed in [11, 13]. Assuming that w is harmonic, the numerical examples in [13] suggest that having (22) and $\left|G_{\rm FIR}(e^{\jmath\Omega})\right| > 0$, for all $\Omega \in \text{spec}(w)$ is sufficient for the performance to converge to zero, and the asymptotic convergence is robust to the choice of tuning parameters η_0 and P_0. It is also shown that (22) is not necessary for zero steady-state error, and, when this condition is not satisfied, an appropriate choice of tuning parameters may still lead to zero asymptotic performance. However, in this case, the asymptotic performance is sensitive to the choice of η_0 and P_0. We stress that (22) is not required for signal boundedness and stability properties, but for the performance to converge to zero.

Two methods for minimizing phase mismatch are presented in [14]. These methods fit the IIR plant G_{zu} with an FIR transfer function $G_{\rm f}$. One method solves a constrained linear least squares problem to bound $\Delta(\Omega)$, while the other method solves a nonlinear least squares problem to minimize $\Delta(\Omega)$ with an FIR fit.

V. Sampling Zeros of the Rohrs Plant

Consider a discrete-time sampled-data system consisting of a zero-order hold, a continuous-time transfer function $T_{zu}(s)$, and a sampler with sampling period h, connected in series. The resulting discrete-time system is characterized by the *pulse transfer function* $G_{zu}(z)$ given by [16]

$$G_{zu}(z) = (1 - z^{-1})\mathcal{Z}\{T_{zu}(s)/s\}. \quad (23)$$

If the relative degree of $T_{zu}(s)$ is at least 2, then $G_{zu}(z)$ has more zeros than $T_{zu}(s)$. The additional zeros are called *sampling zeros* [15].

Proposition 5.1: Let $T_{zu}(s)$ be the $n^{\rm th}$-order rational transfer function

$$T_{zu}(s) = H\frac{(s - z_1)\dots(s - z_m)}{(s - p_1)\dots(s - p_n)} \quad (24)$$

with relative degree $d = n - m \geq 2$, and let $G_{zu}(z)$ be the corresponding pulse transfer function. Then, as the sampling period h approaches 0, $n - d$ zeros of $G_{zu}(z)$ approach 1, and the remaining $d - 1$ zeros of $G_{zu}(z)$ approach the roots of $B_d(z)$, where

$$B_d(z) \triangleq \beta_{d,1}z^{d-1} + \beta_{d,2}z^{d-2} + \dots + \beta_{d,d}, \quad (25)$$

and for $k \in \{1, \dots, d\}$,

$$\beta_{d,k} \triangleq \sum_{i=1}^{k}(-1)^{k-j}i^d \left(\begin{array}{c} d+1 \\ k-i \end{array} \right). \quad (26)$$

Proof 5.1: See Theorem 1 of [15]. □

All of the zeros of $B_d(z)$ are negative, and $B_d(z)$ has at least one zero that is on or outside the unit circle [17]. For $d \geq 3$, $B_d(z)$ has at least one zero outside the unit circle.

As a consequence of Proposition 5.1, sampled-data systems are typically NMP. In particular, for sufficiently small h, the pulse transfer function for a continuous-time system whose relative degree is at least 3 is NMP.

We now discuss the complications that arise in sampled-data control of the Rohrs counterexamples due to unmodeled high-frequency dynamics. In Section IV, the NMP-zero-based construction of $G_{\rm f}$ requires knowledge of the NMP zeros of $G_{zu}(z)$, rather than the NMP zeros of $T_{zu}(s)$. Therefore, we consider the pulse transfer function $G_{zu}(z)$.

We consider the first-order transfer function $T_0(s) = \frac{2}{s+1}$ cascaded with the unmodeled high-frequency dynamics

$$\Lambda(s) = \frac{229}{(s - 15 - \jmath 2)(s - 15 + \jmath 2)}.$$

The plant is given by $T_{zu}(s) \triangleq T_0(s)\Lambda(s)$, which is minimum phase. Although the phase of $T_0(\jmath\omega)$ is in $[0,\ 90]$ deg for all ω, $T_{zu}(\jmath\omega)$ has a phase crossover frequency of $\omega_{pc} = 16.1$ rad/sec.

Since the relative degree of $T_0(s)$ is 1, the pulse transfer function $G_0(z)$ has no sampling zeros for every sampling period h, and thus, $G_0(z)$ is minimum phase. However, due to the unmodeled dynamics $\Lambda(s)$, the relative degree of the plant $T_{zu}(s)$ is 3. Therefore, in accordance with Proposition 5.1, $G_{zu}(z)$ is NMP for all sufficiently small h.

Applying (23) into $T_0(s)$ and $T_{zu}(s)$, the numerator polynomial corresponding to the pulse transfer functions $G_0(z) = N_0(z)/D_0(z)$ and $G_{zu}(z) = N_{zu}(z)/D_{zu}(z)$ are

$$N_0(z) = 2(1 - e^{-h}), \quad (27)$$

$$N_{zu}(z) = \beta_2 z^2 + \beta_1 z + \beta_0, \quad (28)$$

where

$$\beta_0 = -2e^{-31h} + 2.29e^{-30h} + 1.03e^{-16h}\sin 2h - 0.29e^{-16h}\cos 2h, \quad (29)$$

$$\beta_1 = -0.29e^{-30h} + 4.29(e^{-16h} - e^{-15h})\cos 2h + 0.29e^{-h} - 1.03e^{-15h}\sin 2h, \quad (30)$$

$$\beta_2 = 0.29e^{-15h}\cos 2h - 2.29e^{-h} + 2 + 1.03e^{-15h}\sin 2h. \quad (31)$$

Figure 2 illustrates the zeros of (28). We observe that for all $h \lesssim 0.2$, one of the sampling zeros is outside the unit circle and thus $G_{zu}(z)$ has an unknown NMP zero, which is caused by the high-frequency dynamics $\Lambda(s)$. Neither the

presence nor the location of this NMP zero can be assumed to be known. because $\Lambda(s)$ is assumed to be unmodeled.

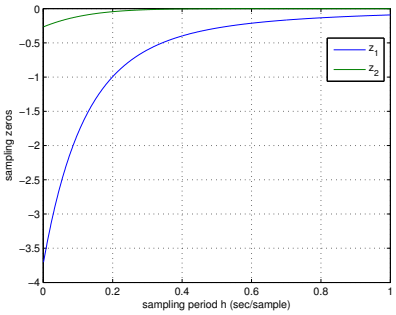

Fig. 2. Sampling Zeros of $G_{zu}(z)$ as a function of h.

VI. Robustness of RCAC for the Rohrs Counterexamples

For $h > 0.2$ sec, the Rohrs sampled-data plant $G_{zu}(z)$ is minimum phase. In this case, for $\eta_0 = 0$, the robustness of NMP-zero-based construction is determined by the ratio of the first Markov parameters of $G_0(z)$ and $G_{zu}(z)$, as discussed in Section IV-A. In Figure 3, we illustrate the first Markov parameters $H_{0,1} = 2(1 - e^{-h})$ and $H_{zu,1} = \beta_2$ of $G_0(z)$ and $G_{zu}(z)$ for $h \in [0, 5]$. As $h \to \infty$, it follows from (27), (31) that both Markov parameters approach 2. Therefore, $\frac{H_{0,1}}{H_{zu,1}} \geq 0.5$ for all h. Hence, the Markov parameter uncertainty is not a robustness issue for the adaptive system. However, for $h \lesssim 0.2$, the available model $G_0(z)$ does not capture the NMP sampling zeros, and therefore, NMP-zero-based construction will not work.

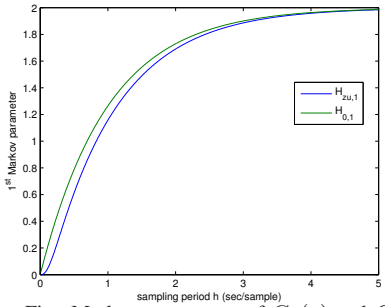

Fig. 3. First Markov parameters of $G_0(z)$ and $G_{zu}(z)$.

On the other hand, using the error-dependent control penalty $\eta(k)$ (17) with $\eta_0 > 0$ ensures robustness and closed-loop stability, whether $G_{zu}(z)$ is NMP or not. Intuitively, closed-loop stability is expected with $\eta_0 > 0$. Indeed, suppose that the closed-loop system becomes unstable, and $z(k)$ diverges to infinity. In this case, the term $\sum_{i=1}^{k} \lambda^{k-i}\eta(i)\hat{\Theta}(k)^{\mathrm{T}}\Phi_{\mathrm{f}}^{\mathrm{T}}(i-1)\Phi_{\mathrm{f}}(i-1)\hat{\Theta}(k)$ in (16) starts dominating other terms. Therefore, assuming $\sum_{i=1}^{k} \Phi_{\mathrm{f}}^{\mathrm{T}}(i-1)\Phi_{\mathrm{f}}(i-1) \geq \alpha I > 0$, the optimization problem reduces to $\min_{\hat{\Theta}(k)} \|\hat{\Theta}(k)\|$, which gives $\hat{\Theta} = 0$. Thus, the closed-loop system reverts back to open-loop. Since the open-loop plant is asymptotically stable, $z(k)$ cannot diverge to infinity, which contradicts the assumption that the closed-loop system is unstable.

Since closed-loop stability does not imply zero asymptotic performance, using $\eta_0 > 0$ does not guarantee zero asymptotic performance. For zero performance, we use phase-matching-based construction to satisfy (22). Since $T_0(s)$ and $T_{zu}(s)$ may have a phase difference larger than 90 deg at high frequencies, fitting an FIR plant with $G_0(z)$ may result in poor phase matching at high frequencies. However, as discussed in Section IV-B, (22) is not a necessary condition for zero steady-state error.

VII. Sampled-Data Adaptive Control of the Rohrs Counterexamples with RCAC

We now apply RCAC to the Rohrs counterexamples [1]. In each example, the goal is to follow the output of the reference model $G_{\mathrm{m}}(s) = \frac{3}{s+3}$. Each simulation is initialized with the controller gain vector $\Theta(0)$ set to zero, and RCAC is turned on at $k = 5$. We use $\lambda = 1$ in all simulations. For consistency with the MRAC architecture, we use the measurements of the plant output y_0 and the reference signal r so that $y = \begin{bmatrix} y_0 & r \end{bmatrix}^{\mathrm{T}}$. All modeling information we use is based on $G_0(z)$ rather than $G_{zu}(z)$. In each case, we illustrate the time traces of $z(k)$, $u(k)$, $\Theta(k)$, and the closed-loop spectral radius $\mathrm{spr}(\tilde{A}(k))$.

A. First Rohrs Counterexample: Sinusoidal Reference Inputs

In this section, we provide simulation results that illustrate the effectiveness of the error-dependent weighting $\eta(k)$ in preserving the closed-loop stability as predicted in Section VI regardless of the frequency content of the reference signal. We first examine the NMP-based construction method with $\eta(k) = 0$, and show that the method exhibits instability when the sampling rate is small enough to cause the sampling zeros to become NMP. We illustrate that the NMP sampling zero is the only cause of instability, and when the sampling period is large, the method does not suffer instability nor any parameter drift, regardless of the frequency spectrum of the reference input. Next, we introduce performance-dependent penalty $\eta(k)$ by letting $\eta_0 > 0$, and show that the closed-loop system remains stable even in the presence of the unknown NMP sampling zero independently of the frequency content of the reference signal.

1) NMP-Zero-Based Construction with $\eta_0 = 0$: We first consider the reference input $r_1(t) = 0.3 + 2\sin(8.0t)$. We sample the continuous-time plant with $h = 0.25$ sec/sample, so that the Nyquist frequency $\omega_{\mathrm{N}} = 4\pi$ rad/sec is larger than the largest reference frequency 8 rad/sec. For this sampling period, the sampling zeros are minimum-phase. The first Markov parameters corresponding to the pulse transfer functions $G_{zu}(z)$ and $G_0(z)$ are $H_{zu,1} = 0.2341$ and $H_{0,1} = 0.4424$, respectively. We let $G_{\mathrm{f}} = H_{0,1}\mathbf{q}^{-1}$, and choose $P_0 = 10I$, $n_{\mathrm{c}} = 10$. As shown in Figure 4, z converges to zero, u remains bounded, Θ converges, and $\mathrm{spr}(\tilde{A})(k)$ converges below 1.

Keeping h the same, we now consider the reference input $r_2(t) = 0.3 + 1.8\sin(16.1t)$, which causes parameter drift and instability in traditional adaptive methods [1]. Note that the frequency of the reference signal is selected at the point where $T_{zu}(s)$ has a 180-deg phase lag. Furthermore, note that the Nyquist rate ω_{N} is smaller than the largest reference frequency 16.1 rad/sec. However, the goal here is to show that closed-loop stability is maintained independently of the

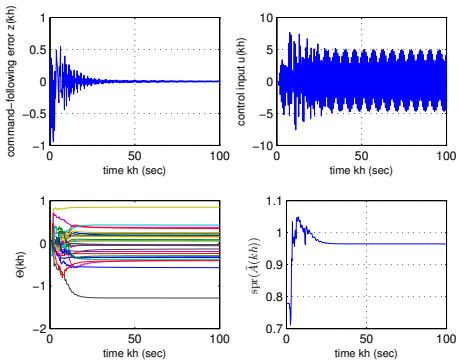

Fig. 4. Response to the reference signal $r_1(t) = 0.3 + 2\sin(8.0t)$ with $h = 0.25$ sec/sample and NMP-zero-based construction with $\eta_0 = 0$.

frequency of the reference command, as long as the sampling zeros arising from the unknown dynamics are minimum-phase. Choosing the same controller and tuning parameters, the parameters converge, and the closed-loop system is stable after convergence as shown in Figure 5. Of course, since h is not small enough to reconstruct $r_2(t)$ from the sampled data, the performance $z(t)$ is not equal to zero between consecutive sampling instants.

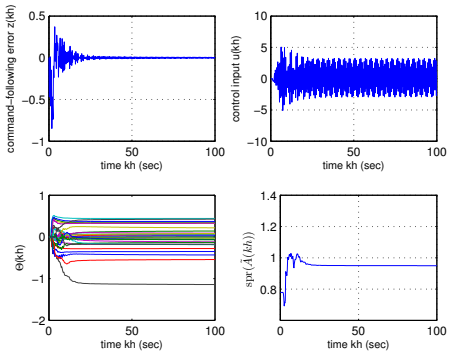

Fig. 5. Response to the reference signal $r_2(k) = 0.3 + 1.8\sin(16.1t)$ with $h = 0.25$ sec/sample and NMP-zero-based construction with $\eta_0 = 0$.

Finally, to improve the intersample behavior, we reduce h to 0.1 sec/sample, and consider $r_2(t)$ again. We have shown in Section VI that $G_{zu}(z)$ is NMP for this sampling rate, and predicted that the choice $G_{\rm f} = H_{0,1}\mathbf{q}^{-1}$ with $\eta_0 = 0$ would lead to instability, since $G_{\rm f}$ does not capture the NMP zeros of G_{zu}. The first Markov parameters are now $H_{zu,1} = 0.037$, $H_{0,1} = 0.1903$, and we choose $G_{\rm f} = H_{0,1}\mathbf{q}^{-1}$, $P_0 = 10I$, and $n_{\rm c} = 10$. RCAC destabilizes the closed-loop system as shown in Figure 6. Similar behavior is obtained with $r_1(t)$ and other reference signals, which confirms that the only cause of instability is the unknown NMP sampling zero.

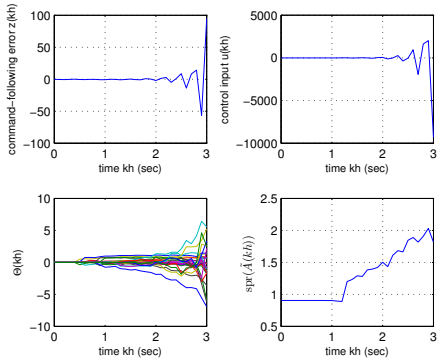

Fig. 6. Response to the reference signal $r_2(t) = 0.3 + 1.8\sin(16.1t)$ with $h = 0.1$ sec/sample and NMP-zero-based construction with $\eta_0 = 0$.

2) Phase-matching-based Construction with $\eta_0 > 0$: We now introduce performance-dependent weighting $\eta(k)$, and use phase-matching-based construction for zero asymptotic performance. We sample the plant with $h = 0.1$ sec/sample. We use the linear fitting method outlined in [14] to obtain $G_{\rm f} = 0.1946\mathbf{q}^{-1} + 0.1761\mathbf{q}^{-2}$, which bounds $\tilde{\Delta}(\Omega)$ by 65 deg from above, where $\tilde{\Delta}(\Omega)$ is defined as in (20) with G_{zu} replaced by G_0. Consequently, this choice does not guarantee (22); in fact, we have $\Delta(\Omega) > 90$ for $\Omega \in [0.6,\ 1.77] \cup [2.73\ \pi]$ rad/sample. Note that the NMP sampling zero -1.82 of G_{zu} is not captured by $G_{\rm f}$.

We first consider $r_1(t)$. We have $\Delta(0) = 0$ deg, and $\Delta(0.8) = 94$ deg at the reference frequencies. Choosing $\eta_0 = 0.3$, $p_c = 10$, $P_0 = I$, and $n_{\rm c} = 10$, z converges to zero, and the asymptotic closed-loop system is stable with no parameter drift as shown in Figure 7.

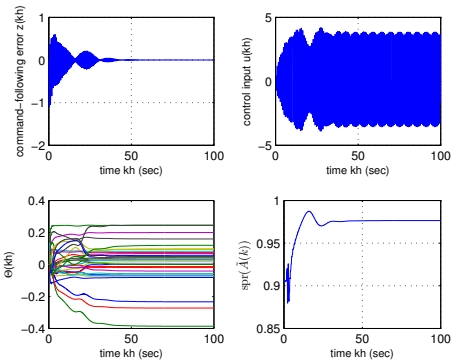

Fig. 7. Response to the reference signal $r_1(t) = 0.3 + 2\sin(8t)$ with $h = 0.1$ sec/sample and phase-matching-based construction with $\eta_0 = 0.3$.

Keeping $G_{\rm f}$, η_0, P_0, and $n_{\rm c}$ the same, we now consider $r_2(t)$. We have $\Delta(1.61) = 92$ deg at the sinusoidal component of the reference spectrum. To ensure that no parameter drift occurs, we simulate the adaptive system for 2000 seconds. The performance converges to zero, and the asymptotic closed-loop system is stable as shown in Fig. 8.

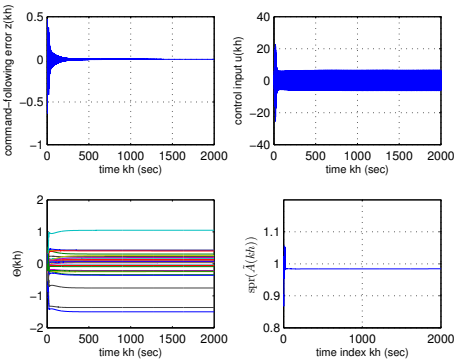

Fig. 8. Response to the reference signal $r_2(t) = 0.3 + 1.8\sin(16.1t)$ with $h = 0.1$ sec/sample and phase-matching-based construction with $\eta_0 = 0.3$.

B. Second Rohrs Counterexample: Sensor Noise and Lack of Persistent Excitation

Unknown additive sensor noise is pointed as the second main robustness challenge for common adaptive methods [1]. In this section, we show that RCAC is unconditionally robust to sensor noise with either construction methods.

We consider the unknown additive sensor noise $d(t)$, and modify the measurement vectors y and z to have

$$y(k) \triangleq \begin{bmatrix} y_0(k) + d(k) & r(k) \end{bmatrix}^{\mathrm{T}},$$
$$z(k) \triangleq \begin{bmatrix} y_0(k) + d(k) - y_{\mathrm{M}}(k) \end{bmatrix}$$

Hence, RCAC interprets the sensor noise as an additional component of the command that needs to be followed. Hence, the performance measurement z is not equal to the command-following error $y_0 - y_{\mathrm{M}}$. For illustration, we consider the step reference input $r(t) = 2$, which is persistently exciting of order one, with the unknown sensor noise $d(t) = 0.5 \sin 8t$, which is persistently exciting of order two.

1) NMP-zero-based Construction with $\eta_0 = 0$: We sample the continuous-time plant $h = 0.25$ sec/sample, and thus the sampling zeros are minimum-phase. Applying RCAC with $G_{\mathrm{f}} = H_{0,1}\mathbf{q}^{-1}$, $n_{\mathrm{c}} = 10$, and $P_0 = 10I$, the performance measurement (not the command-following error) is driven to zero, the parameters converge, and the closed-loop system is stable as shown in Figure 9.

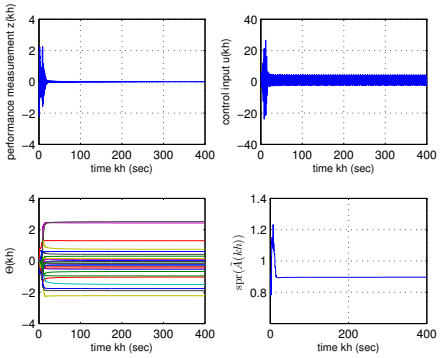

Fig. 9. Response to the reference input $r(t) = 2$ and sensor noise $d(t) = 0.5 \sin 8t$ with $h = 0.25$ sec/sample and NMP-zero-based construction.

2) Phase-matching-based Construction with $\eta_0 > 0$: We now sample the continuous-time plant with $h = 0.1$ sec/sample, and thus one of the sampling zeros is NMP. Applying RCAC with $G_{\mathrm{f}} = 0.1946\mathbf{q}^{-1} + 0.1761\mathbf{q}^{-2}$, $\eta_0 = 0.3$, $p_c = 10$, $P_0 = I$, and $n_{\mathrm{c}} = 10$, z converges to zero, the parameters converge, and the closed-loop system is stable as shown in Figure 10.

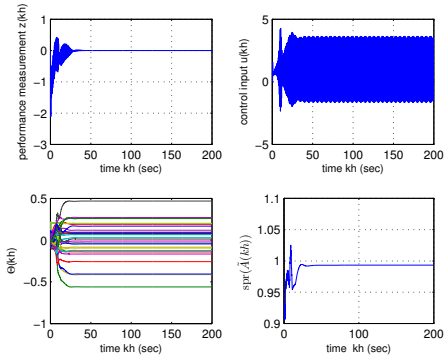

Fig. 10. Response to $r(t) = 2$ and $d(t) = 0.5 \sin 8t$ with $h = 0.1$ sec/sample and phase-matching-based construction with $\eta_0 = 0.3$.

VIII. Conclusions

We revisited the Rohrs counterexamples within the context of sampled-data adaptive control using RCAC algorithm. From a sampled-data point of view, it turns out that the challenging aspect of these problems for RCAC is not the unmodeled dynamics per se, but rather the sampling zeros, which may be NMP under fast sampling. These sampling zeros are induced by the unmodeled dynamics, and thus cannot be assumed to be known. Nevertheless, since the Rohrs counterexamples are open-loop asymptotically stable, with the use of a performance-dependent weighting, RCAC is able to provide reliable performance without the knowledge of either the unmodeled high-frequency dynamics or the NMP sampling zeros, regardless of the frequency content of the reference input. Finally, the presence of output disturbances do not adversely affect the closed-loop stability of the adaptive system, regardless of the degree of persistency of the reference input or the disturbance signal.

References

[1] C. E. Rohrs, L. Valavani, M. Athans, and G. Stein, "Stability Problems of Adaptive Control Algorithms in the Presence of Unmodeled Dynamics," *Conf. Dec. Contr.*, December, 1982.

[2] B. D. O. Anderson, A. Dehghani, "Challenges of Adaptive Control–Past, Permanent and Future," *Annual Reviews in Control*, Vol. 32, pp. 123–135, 2008.

[3] B. D. O. Anderson, "Failures of Adaptive Control Theory and Their Resolution," *Communications in Information and Systems*, Vol. 5, No. 1, pp. 1–20, 2005.

[4] K. J. Astrom and B. Wittenmark, *Adaptive Control*, 2nd ed., Addison-Wesley, 1995.

[5] G. C. Goodwin and K. S. Sin, *Adaptive Filtering, Prediction and Control*, Prentice Hall, 1984.

[6] P.A Ioannou and J. Sun, *Robust Adaptive Control*, Prentice Hall, 1996.

[7] R. Venugopal and D. S. Bernstein, "Adaptive Disturbance Rejection Using ARMARKOV System Representations," *IEEE Trans. Contr. Sys. Tech.*, vol. 8, pp. 257–269, 2000.

[8] J. B. Hoagg, M. A. Santillo, and D. S. Bernstein, "Discrete-Time Adaptive Command Following and Disturbance Rejection for Minimum Phase Systems with Unknown Exogenous Dynamics," *IEEE Trans. Autom. Contr.*, Vol. 53, pp. 912–928, 2008.

[9] M. A. Santillo and D. S. Bernstein, "Adaptive Control Based on Retrospective Cost Optimization," *AIAA J. Guid. Contr. Dyn.*, Vol. 33, pp. 289–304, 2010.

[10] J. B. Hoagg and D. S. Bernstein, "Retrospective Cost Adaptive Control for Nonminimum-Phase Discrete-Time Systems Part 1: The Ideal Controller and Error System; Part 2: The Adaptive Controller and Stability Analysis," *Proc. Conf. Dec. Contr.*, pp. 893–904, Atlanta, GA, December 2010.

[11] A. M. D'Amato, E. D. Sumer, and D. S. Bernstein, "Frequency-Domain Stability Analysis of Retrospective-Cost Adaptive Control for Systems with Unknown Nonminimum-Phase Zeros," *Proc. Conf. Dec. Contr.*, pp. 1098-1103, Orlando, FL, December 2011.

[12] M. S. Fledderjohn, M. S. Holzel, H. Palanthandalam-Madapusi, R. J. Fuentes, and D. S. Bernstein, "A Comparison of Least Squares Algorithms for Estimating Markov Parameters," *Proc. Amer. Contr. Conf.*, pp. 3735–3740, Baltimore, MD, June 2010.

[13] E. D. Sumer, A. M. D'Amato and D. S. Bernstein, "Robustness of Retrospective-Cost Adaptive Control to Markov-Parameter Uncertainty," *Proc. Conf. Dec. Contr.*, pp.6085–6090, Orlando, FL, December 2011.

[14] E. D. Sumer, M. H. Holzel, A. M. D'Amato, and D. S. Bernstein, "FIR-Based Phase Matching for Robust Retrospective-Cost Adaptive Control," *Proc. Amer. Contr. Conf.*, Montreal, CA, June 2012.

[15] K. J. Astrom, P. Hagander, and J. Sternby, "Zeros of Sampled Systems," *IEEE Trans. Autom. Contr.*, Vol. 20, No. 1, pp. 31–38, 1984.

[16] B. C. Kuo, *Digital Control Systems*, HRW, 1980.

[17] S. R. Weller, W. Moran, B. Ninness, and A. D. Pollington, "Sampling zeros and the Euler-Frobenius polynomials," *IEEE Trans. Automatic Contr.*, Vol. 46. No. 2, pp. 340-343, 2001.